

Circ_0007386 Promotes the Progression of Hepatocellular Carcinoma Through the miR-507/CCNT2 Axis

Yanzhi Feng^{1-4,*}, Litao Liang^{1-4,*}, Wenbo Jia¹⁻⁴, Jinyi Wang¹⁻⁴, Chao Xu¹⁻⁴, Deming Zhu¹⁻⁴, Bin Xu¹⁻⁴, Wenhui Zhao¹⁻⁴, Xiangyu Ling¹⁻⁴, Yongping Zhou⁵, Lianbao Kong^{1-4,*} , Wenzhou Ding^{1-4,*}

¹Hepatobiliary Center, the First Affiliated Hospital of Nanjing Medical University, Nanjing, Jiangsu, People's Republic of China; ²Key Laboratory of Liver Transplantation, Chinese Academy of Medical Sciences, National Health Commission Key Laboratory of Living Donor Liver Transplantation (Nanjing Medical University), Nanjing, Jiangsu, People's Republic of China; ³Jiangsu Provincial Medical Innovation Center, Nanjing, Jiangsu, People's Republic of China; ⁴Jiangsu Provincial Medical Key Laboratory, Nanjing, Jiangsu, People's Republic of China; ⁵Jiangnan University Medical Center, JUMC, Department of Hepatobiliary, Wuxi, Jiangsu, People's Republic of China

*These authors contributed equally to this work

Correspondence: Wenzhou Ding; Lianbao Kong, Hepatobiliary Centre, The First Affiliated Hospital of Nanjing Medical University, 300 Guangzhou Road, Nanjing, 210029, People's Republic of China, Email dingwenzhou@njmu.edu.cn; lbkong@njmu.edu.cn

Background: Circular RNAs (circRNAs) have been shown to play a crucial role in the initiation and development of Hepatocellular carcinoma (HCC). However, the mechanism and function of circ_0007386 in HCC are still unknown.

Methods: Circ_0007386 expression level in HCC tissues, and HCC cell lines was further analyzed by qRT-PCR. Agarose gel electrophoresis and Sanger sequencing were used to figure out the structure of circ_0007386. The involvement of circ_0007386 in HCC development was evaluated by experimental investigations conducted in both laboratory settings (in vitro) and living organisms (in vivo). RNA immunoprecipitation, Western blotting, luciferase reporter assay and fluorescence in situ hybridization (FISH) were applied for finding out the interaction among circ_0007386, miR-507 and CCNT2. To assess the connection between circ_0007386 and lenvatinib resistance, lenvatinib-resistant HCC cell lines were employed.

Results: The expression of circ_0007386 was found to increase in HCC tissues, and it was observed to be associated with a worse prognosis. Overexpression of circ_0007386 stimulated HCC cells proliferation, invasion, migration and the epithelial-mesenchymal transition (EMT) while silencing of circ_0007386 resulted in the opposite effect. Mechanistic investigations revealed that circ_0007386 acted as a competing endogenous RNA of miR-507 to prevent CCNT2 downregulation. Downregulating miR-507 or overexpressing CCNT2 could reverse phenotypic alterations that originated from inhibiting of circ_0007386. Importantly, circ_0007386 determines the resistance of hepatoma cells to lenvatinib treatment.

Conclusion: Circ_0007386 advanced HCC progression and lenvatinib resistance through the miR-507/CCNT2 axis. Meanwhile, circ_0007386 served as a potential biomarker and therapeutic target in HCC patients.

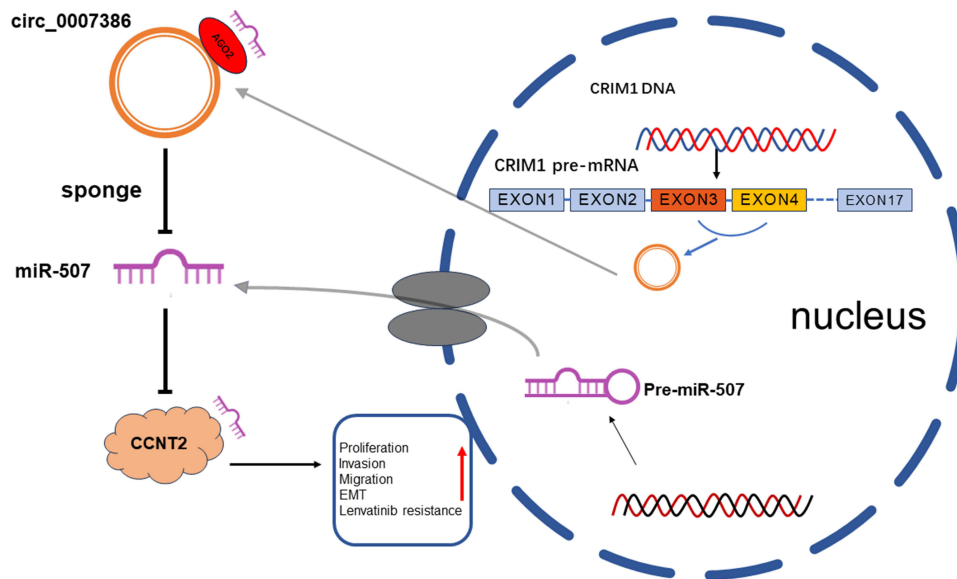
Keywords: hepatocellular carcinoma, circ_0007386, miR-507, CCNT2, Lenvatinib

Introduction

Hepatocellular cancer (HCC) is the fourth leading cause of cancer death worldwide and the second largest cause of impaired cancer life expectancy worldwide, which emphasizes the significant disease burden of liver cancer.¹ The treatment of HCC is a full-spectrum therapy modality based on aggressive resection, whereas there are no effective molecular therapeutic targets. Despite various attempts to improve treatment choices, HCC still has a dismal prognosis.² Therefore, research on the genetic and molecular basis of HCC development is critical.

Circular RNAs (circRNAs), noncoding RNAs (ncRNAs), are regarded as modulators of gene expression, m6A modification and RNA binding proteins. Furthermore, current studies have demonstrated that circRNAs can behave as

Graphical Abstract



molecular sponges for miRNA regulation and interact with RNA-binding proteins to modulate transcriptional processes.³⁻⁵ An increasing number of circRNAs have been linked to tumor growth, suggesting that they may play a crucial role in the pathogenesis of many different tumor types.⁶⁻⁸ The above findings suggest that circRNAs hold significant research potential. Nevertheless, a considerable number of circRNAs remain to be identified and investigated.

Studies have demonstrated the significance of circRNAs produced from CRIM1 in a variety of carcinomas, including bladder cancer, ovarian cancer, and nasopharyngeal carcinoma.⁹⁻¹¹ However, the function of circRNAs derived from CRIM1 in HCC has rarely been reported.¹² Through database analysis, we found that circRNAs derived from CRIM1, especially circ_0007386, show substantial expression differences in HCC and paraneoplastic tissues. Our data demonstrate a considerable upregulation of circ_0007386 in HCC tissue and cell lineages and that elevated levels of circ_0007386 are associated with a poor prognosis in HCC patients. Furthermore, our findings indicate that circ_0007386 plays a significant role in the progression of HCC by upregulating CCNT2 as a miR-507 sponge. Importantly, we found that circ_0007386 can decrease the sensitivity of HCC cells to lenvatinib. Hence, the outcomes of this investigation suggest that circ_0007386 exhibits carcinogenic properties, potentially serving as a prognostic indicator for the advancement of HCC and the efficacy of chemotherapy.

Materials and Methods

Cell Culture and Clinical Specimens

From the Chinese Academy of Sciences Cell Bank (CASCB, Shanghai, China), we obtained all HCC cells and normal human liver cells (HHL-5). All cells were grown in Dulbecco's Modified Eagle medium (DMEM, Gibco, NY, USA) containing 10% fetal bovine serum (Gibco), 50 U/mL penicillin and 50 U/mL streptomycin (Invitrogen, CA, USA). The cells grow in moistened containers containing 5% CO₂ and are used after cells enter the index growth phase.

All HCC tissue and normal liver tissue alongside cancer were obtained from patients undergoing surgical treatment at the Hepatobiliary Center of the First Affiliated Hospital of Nanjing Medical University. All patients in the study had been clinically diagnosed with tissue pathology, but none had any prior therapeutic interventions. Before any tissue samples were obtained, patients gave their consent after receiving all relevant information. The study was conducted in accordance with the Declaration of Helsinki, and approved by the Ethics Committee of the First Affiliated Hospital of Nanjing Medical University (2022-SRFA-221).

Generation of Lenvatinib-resistant Cells

MHCC97H and Hep3B were exposed to graded drug concentrations (5 mol/L to 25 mol/L) to generate lenvatinib resistance. The establishment of two HCC cell lines resistant to lenvatinib was achieved during a four-month induction period.

Quantitative RT-PCR Analysis (qRT-PCR)

All RNA was extracted from the cells by TRIzol reagent (Invitrogen) and quantified using a NanoDrop ND-1000. To perform qRT-PCR, the RNA was reverted to cDNA using a reverse transcription kit (Vazyme, Nanjing, China). We used AceQ qPCR SYBR Green Master Mix (Vazyme) and an ABI 7900 PCR system (Applied Biosystems, CA, USA) for real-time quantitative PCR analysis. Glycol-aldehyde-3-phosphate dehydrase (GAPDH) is an inherent contrast between circRNA and mRNA, while U6 is the intrinsic contrast of miRNA. The primers used in this study are included in the Supplementary Information ([Table S1](#)).

Cell Transfection

Before transfection, MHCC97H and Hep3B cells were incubated in a 6-well plate and cultivated to 60–70% confluence. We transfected the cells with Lipofectamine 3000 (Invitrogen) according to the manufacturer's instructions. CircRNA (hsa_circ_0007386) overexpressing plasmid (p-circRNA) and small interfering RNA (siRNA) targeting circ_0007386, miR-507 mimic and inhibitor, overexpressed plasma CCNT2 and Si-CCNT2 as well as nonspecific negative control oligonucleotides (si-control), and negative control (NC) were purchased from RIBOBIO (Guangzhou, China). The lentivirus targeting hsa_circ_0007386 was purchased from GeneChem (Shanghai, China).

RNase R and Actinomycin D Assays

Total RNA (2 g/group) was extracted from cells and treated for 30 minutes at 37 °C with 3 U/g RNase R (Epicenter Technologies, Madison, WI, USA). It was purified using a RNeasy MinElute Cleaning Kit (Qiagen, Germantown, MD, USA). Following that, the quantity of Circ_0007386 and GAPDH mRNA was determined using qRT-PCR.

Cells were treated with 5 g/mL actinomycin D (Sigma Aldrich, St. Louis, MO, USA) to inhibit gene transcription. The cells were then taken at indicated time points (0, 4, 8, 12, and 24 hours) and total RNA was extracted. qRT-PCR was used to determine the relative expression levels of circ_0007386 and CRIM1, as well as their half-lives.

Cell Counting Kit-8 Proliferation Assay

The cells were distributed onto 96-well plates, with each well containing 1000 cells suspended in 100 µL of the medium. After 1, 2, 3, 4, and 5 days, 10µL of CCK8 solution (TransGene, Beijing, China) was added to each well. The plate was incubated for 2 hours at a temperature of 37 degrees Celsius. Finally, it was analyzed using a spectrophotometer (Thermo Scientific, Pittsburgh, PA, USA) set to a wavelength of 450 nm.

Colony Formation

Approximately 500 cells were seeded into each well of a 6-well plate. After two weeks, we cleaned each well with phosphate-buffered saline (PBS) and fixed the cells with 4% paraformaldehyde. After that, cells were stained with crystal violet (Beyotime, Shanghai, China). Colonies were counted visually.

Transwell Migration and Invasion Assay

About 3×10^4 cells were planted on the upper chamber after being suspended in 300ul FBS-free medium for the migration assay. The lower chamber received 600ul of medium containing 10% FBS. The cells were treated with a 4% paraformaldehyde solution for fixation and subsequently stained with crystal violet following an incubation period of about 48 hours. Cotton swabs were used to scrape off the upper layer of cells. Then we recorded the results using a microscope on the chambers. In cell invasion assay, the upper layer was covered with Matrigel matrix (BD Biosciences, Franklin Lakes, NJ, USA). The subsequent procedures were identical to those employed in the cell migration assay.

Edu Assay

An EdU kit (Beyotime) was used for the proliferation assay. In brief, 10,000 cells were seeded into each well of a 96-well plate, cultivated for 12 hours, and then treated with EdU for 2 hours. According to the protocol, 300 μ L of Apollo dyeing solution was added to each well. Each well had 300 μ L of a 1:100 dilution of Hoechst reaction solution in deionized water added to it. Images were taken with a fluorescence microscope.

Wound Healing Assay

When the cell confluence reached 90%, a 200 μ L pipette was used to draw a vertical line along the center of the plate. The cells grew in a medium devoid of FBS. At 0 hours, 24 hours, and 48 hours, the identical areas of cell migration were photographed.

Agarose Gel Electrophoresis

We amplified cDNA and gDNA from HCC cell lines using Circ_0007386 primers that were divergent and convergent (RiboBio, Guangzhou, China). Then we collected the amplified products. The amplified products were electrophoresed in an agarose gel with 1% agarose solution (Beyotime), and the band location was examined under ultraviolet light.

Fluorescence in situ Hybridization (FISH)

Briefly, after prehybridization at 55 °C for 2 h, cells were hybridized with a specific Cy3-labeled circ_0007386 probe and 18S probe, and U6 probe (RiboBio) at 37 °C overnight and dyed with 4', 6-diamidino-2-phenylindole (DAPI). Images were taken with a confocal laser microscope.

Immunofluorescence

HCC cells cultivated on cell climbing pieces underwent two rounds of rinsing with PBS and subsequently fixed with a 4% solution of paraformaldehyde for 15 minutes. After washing the cells with PBS, Triton was added and left on ice for 10 minutes to lyse the cells. The cells were then blocked with goat serum for 30 minutes at 37 °C, and treated overnight at 4 °C with primary anti-E-cadherin (Proteintech), anti-N-cadherin (Proteintech), and anti-Vimentin (Servicebio) antibodies. After washing with PBS, the cells were incubated with the corresponding secondary antibody for 45 min at room temperature. Then, DAPI (Beyotime) was used to stain the nuclei of the cells. A confocal microscope was used to take pictures of fluorescence images.

Dual-Luciferase Reporter Assay

The binding sites between Circ_0007386 and miR-507 were predicted by the Circinteractome database and the binding sites of miR-507 and the CCNT2 3'UTR were predicted by the TargetScan database. Wild-type (WT) and mutant-type (MUT) particles were designed. HEK-293T cells were spread 24 hours in advance with 5×10^4 per well into 24 well cell culture plates. Transfection reagents were used to cotransfect wild-type or mutant vectors with miRNA mimics/NC into cells. Meanwhile we added 5ng of sea kidney luciferase vector to the Petri plate. After 24 hours, we discarded the waste, added 150 μ L of potassium clotting solution (PLB) to the Petri plate, and incubated the plate on ice for 20 min. Luciferase activity was measured and quantified using a dual luciferase reporter gene assay system (Promega, Madison, WI, USA).

Tumor Xenografts and Pulmonary Metastasis in Mice

From the Model Animal Research Center of Nanjing Medical University (NJMU), we obtained four-week-old male BALB/c nude mice. These mice were randomly divided into four different groups of six each. Two of these groups were subcutaneously infected with MHCC97H cells infected with sh-circ_0007386 or sh-NC, while the other two groups were subcutaneously infected with Hep3B cells transfected with Lv-circ_0007386 or Lv-NC. Lentivirus transfected cells were suspended in PBS at a cell density of 1×10^8 /mL; 100 μ L of cell suspension was injected under the skin of each mouse's upper-left femur; we recorded the volume of the subcutaneous tumor every 3 days. Volume (mm^3) = $0.5 \times \text{length} \times \text{width}^2$.

After thirty days, we euthanized the mice, removed their subcutaneous tumors, measured their size and mass, and took photographs of them.

Transfected cells were injected into the tail vein of other mice which were randomly separated into four groups to establish a lung metastasis model. After six weeks, we euthanized nude mice, removed lung tissue to count tumors, and took photographs.

All experiments were repeated three times. Some of the tumors were then preserved in formaldehyde for subsequent immunohistochemistry and hematoxylin and eosin (H&E) staining. The animal study protocol was approved by Institutional Animal Care and Use Committee of the First Affiliated Hospital of Nanjing Medical University (IACUC-2305004).

RNA Immunoprecipitation (RIP)

To investigate whether circ_0007386 and miR-507 bind to the Ago2 protein, we first incubated cell lysates at 4 °C with magnetic beads attached to Ago2 antibody or IgG, and then repeated incubations with proteinase K to remove the protein. Finally, the RNA was extracted for RT-PCR analysis.

Western Blotting

Proteins were extracted utilizing RIPA buffer (Beyotime) supplemented with protease inhibitors. In accordance with the protocol, the extracted protein was first separated by 10% SDS-PAGE and subsequently transferred onto a polyvinylidene fluoride membrane (Merck Millipore, Burlington, MA, USA). After incubating the membranes with the primary antibodies at 4 °C overnight, they were blocked with rapid blocking buffer (Beyotime) for 50 minutes. Following a 2 hour incubation with the corresponding secondary antibodies and three 10-minute washes in Tris-buffered saline + Tween (TBST), the protein content was visualized with Image Lab software (Bio-Rad, Hercules, CA, USA) and a hypersensitive ECL exposure solution. The primary antibodies used in this experiment were as follows: GAPDH (Proteintech, Wuhan, China), E-cadherin (Proteintech), N-cadherin (Proteintech), vimentin (Servicebio), and CCNT2 (Bioss, Beijing).

Pull-Down Assay with Biotinylated miRNA

The probe was designed to bind to the junction area of circ_0007386. After cells were lysed, 3 mg of biotinylated probes was incubated with pyrolysis products at room temperature for 2 hours. Then the mixture was incubated with 50 mL streptavidin-conjugated magnetic beads at RT for 4 h. The RNA was extracted by adding TRIzol LS (Invitrogen, Thermo, USA) following several cycles of washing beads. The RNA was reverse-transcribed using a miRNA First-Strand Synthesis kit (Clontech, Takara, Japan) and analyzed by qRT-PCR analysis.

Statistical Analysis

All data are expressed as the mean \pm standard difference (SD) and $p < 0.05$ is considered significant. GraphPad Prism software v8.0 (GraphPad, San Diego, CA, USA) was used to perform statistical analysis. If the differences between the groups followed a normal distribution, the Student's *t*-test was applied to make comparisons; otherwise, the Mann-Whitney *U*-test was utilized. One-way analysis of variance was performed to compare three groups. For survival analysis, the KM method (Log rank test) was performed for univariate analysis, and the stepwise Cox multivariate proportional hazard regression model (Forward LR, likelihood ratio) was executed for multivariate analysis. Correlations were tested by Spearman correlation test.

Results

Circ_0007386 is Highly Expressed in HCC

Primers for eight CRIM1-derived circRNAs were created to learn more about their function in HCC. qRT-PCR analysis of circRNAs derived from CRIM1 in 10 pairs of HCC and paracarcinoma tissues revealed that circ_0007386 and circ_0002346 are upregulated in HCC (Figure 1A and B). We then separately evaluated the expression of circ_0007386

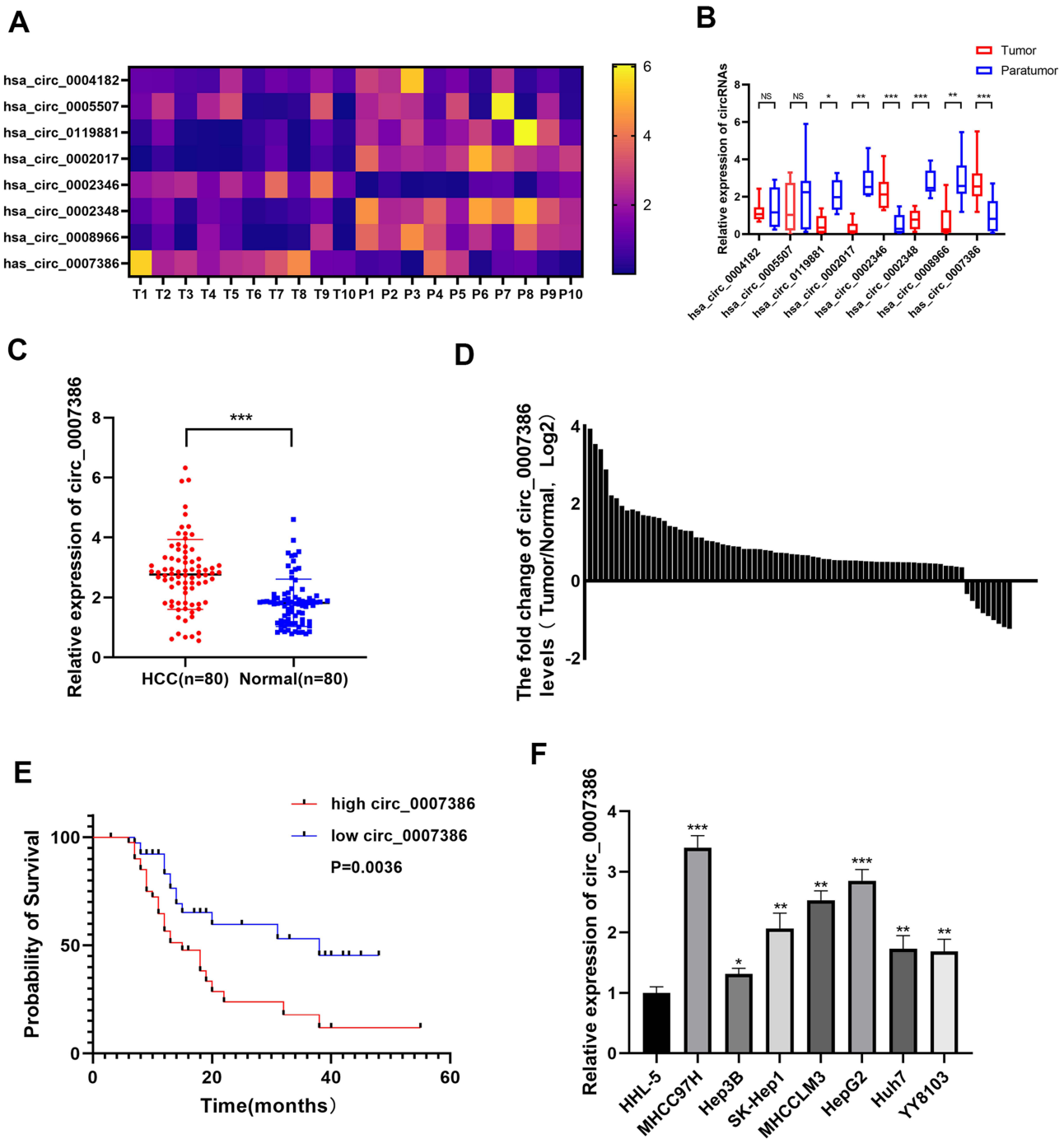


Figure 1 Hsa_circ_0007386 is highly expressed in HCC tissues compared to other circRNAs derived from CRIM1. (A–B) The expression of 8 CRIM1-derived circRNAs in 10 pairs of HCC and para carcinoma tissues were detected by qRT-PCR. (C) The relative expression level of hsa_circ_0007386 in HCC tissues and matched para-cancer tissues (n = 80) was measured using qRT-PCR. (D) Kaplan–Meier survival curves of HCC patients with low and high hsa_circ_0007386 expression. (E) The fold change of hsa_circ_0007386 expression between HCC and paratumor tissues. (F) Expression of circ_0007386 in various cell lines. Data were all showed as mean ± SD; ns indicated no significance, *p < 0.05, **p < 0.01, ***p < 0.001.

and circ_0002346 in 80 pairs of HCC and paracarcinoma tissues and found that circ_0007386 expression was significantly elevated in HCC (Figure 1C and D, Figure S1A). To assess the clinical significance of circ_0007386, the cohort of 80 HCC patients was divided into two groups based on the median level of circ_0007386 expression (Table 1). Our data suggested that the expression of circ_0007386 exhibited a positive correlation with tumor volume, TNM stage, and vascular invasion in patients with HCC, as evaluated via clinicopathological examination; however, no statistical

Table I Relationship Between Circ_0007386 Expression Level in HCC Tissues and Clinical Parameters of Patients

Clinical Parameters		total	Circ_0007386		P value
			High Group	Low Group	
Age (years)	>60	48	26	22	0.4327
	≤60	32	16	16	
Gender	male	43	22	21	0.4815
	female	37	20	17	
Tumor size (cm)	≤5	49	26	23	0.0014
	>5	31	23	8	
TNM stage	I	48	25	23	0.0032
	II–III	32	23	9	
Vascular invasion	Yes	45	24	21	0.0007
	No	35	26	9	
AFP (ng/mL)	<400	31	18	13	0.0572
	≥400	49	22	27	
HBsAg	Negative	17	7	10	0.1035
	Positive	63	35	28	

Abbreviations: AFP, alpha fetoprotein; HBsAg, hepatitis B surface antigen.

significance for age, sex, AFP or HBsAg was observed. The Kaplan–Meier analysis of survival revealed that patients with higher levels of circ_0007386 had a shorter overall survival time (Figure 1E). Finally, qRT-PCR was employed to validate the higher expression of circ_0007386 in HCC cells than in normal liver cells (HHL-5) (Figure 1F).

Confirmation of Circ_0007386 Characteristics

Circ_0007386 is derived from exons 3–4 of the CRIM1 gene. (Figure 2A) The backsplicing locations of circ_0007386 were validated by Sanger sequencing, which also differentiated circ_0007386 from a lariat RNA. (Figure 2B) In addition, divergent primers and convergent primers were designed to amplify circ_0007386 linear mRNA and circ_0007386 from HCC cells using cDNA and genomic DNA (gDNA). Agarose gel electrophoresis showed that circ_0007386 linear mRNA could be detected in both cDNA and gDNA, while circ_0007386 could be detected in only cDNA and not in gDNA (Figure 2C). RNase R and actinomycin D treatment assays were performed to validate that circ_0007386 had higher stability than linear CRIM1 mRNA (Figure 2D and E). Because circRNAs play different roles in different parts of the cell, we conducted nucleoplasmic separation experiments and a FISH assay to validate that circ_0007386 is mostly localized in the cytoplasm before making any predictions about its function. (Figure 2F and G)

Circ_0007386 Promoted the Proliferation, Migration and Invasion of HCC Cells

To ensure that circ_0007386 is involved in the proliferation of HCC, a series of functional assays was conducted on the HCC cell line. Initially, the expression of circ_0007386 was inhibited in MHCC97H cells and upregulated in Hep3B cells through lentiviral transfection. Since the expression of circ_0007386 in MHCC97H was the highest, while that of Hep3B was the lowest. The efficacy of transfection was evaluated through the utilization of PCR (Figures 3A and S1B). To examine the proliferation of cells, our study employed various experimental techniques, including CCK-8, EdU, and colony formation assays (Figures 3B, C and S1C). The results demonstrated that circ_0007386 knockdown substantially inhibited the proliferation of MHCC97H cells, but opposite findings were observed in Hep3B cells overexpressing circ_0007386. Wound-healing and transwell experiments were carried out to further examine the effect of circ_0007386 on HCC cell invasion and migration. (Figures 3D and S1D) Investigations showed that circ_0007386 overexpression considerably increased the ability of HCC cells to migrate and invade, while circ_0007386 inhibition significantly decreased these capacities. These results demonstrated that circ_0007386 increases the proliferation and motility of HCC

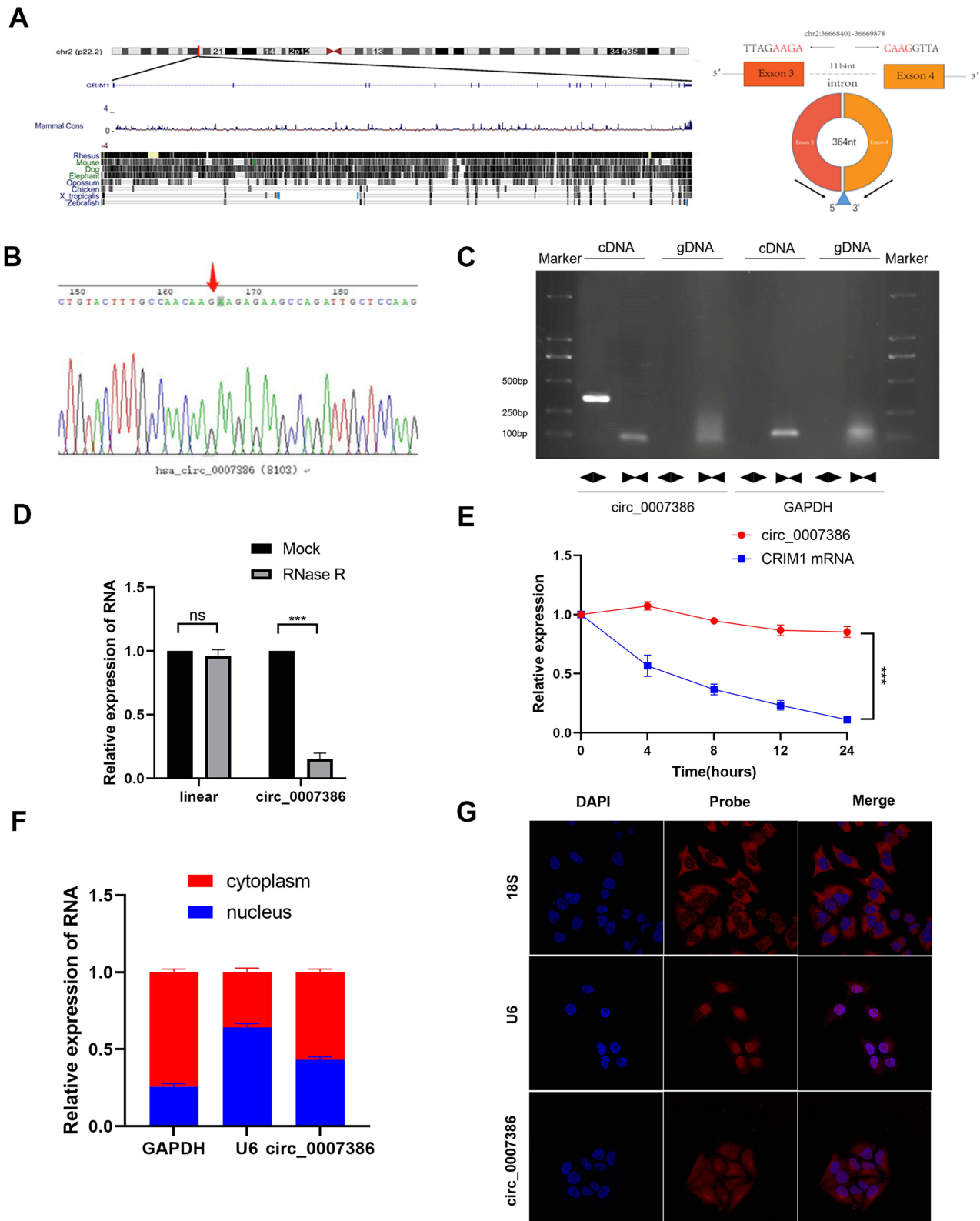


Figure 2 Confirmation of the circular structure of circ_0007386. (A) The schematic illustration depicted the circularization of CRIM1 exon 3 to 4 into circ_000007386. (B) Sanger sequencing revealed circ_0007386's splicing site. (C) RT-PCR and agarose gel electrophoresis confirmed the existence of circ_0007386 in HCC cell. (D–E) The expression of circ_0007386 and CRIM1 mRNA in HCC cells were detected by qRT-PCR with RNase R and actinomycin D. (F–G) The FISH assay and Cyto-plasmic separation experiment revealed that circ_0007386 is mainly situated in the cytoplasm. Data were all showed as mean ± SD; ns indicated no significance, *p < 0.05, ***p < 0.001.

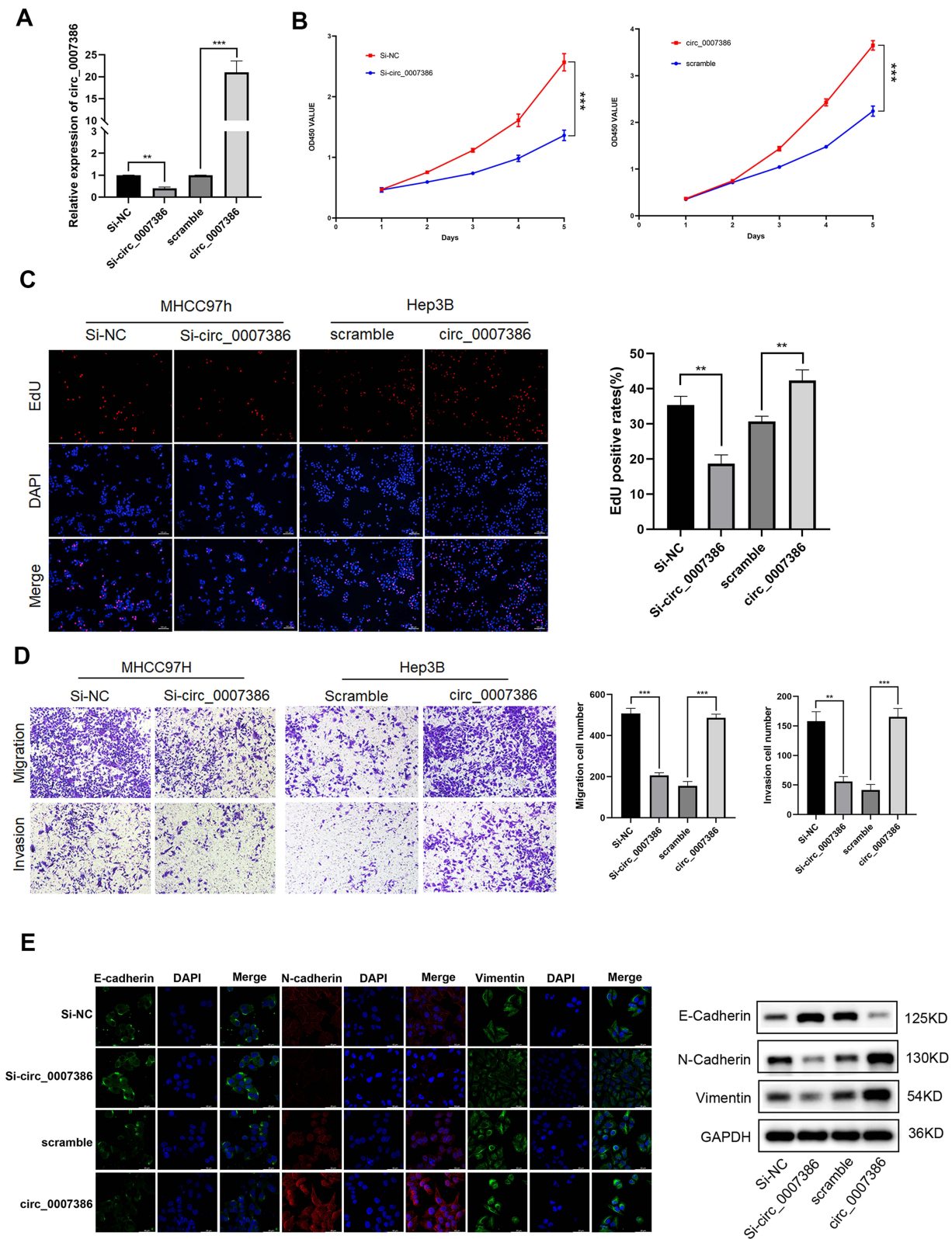


Figure 3 Circ_0007386 promoted the proliferation, invasion, migration and induces the EMT of HCC cells in vitro. MHCC97H was transfected with si-NC or si-circ, and Hep3B was transfected with scramble or oe-circ. (A) The knockdown and overexpression efficiency of circ_0007386 in HCC cells were determined by qRT-PCR. (B–C) CCK-8 assays and EdU assays were used to evaluate the proliferative capabilities of HCC cells. (D) Transwell assays was used to evaluate the migratory and invasive ability of HCC cells. (E) Western blot and immunofluorescence was used to detect EMT-related proteins after suppression or overexpression of circ_0007386. Data were all showed as mean ± SD; ns indicated no significance, **p < 0.01, ***p < 0.001.

cells. Western blotting and immunofluorescence indicated that circ_0007386 promotes epithelial–mesenchymal transformation (EMT) in HCC (Figure 3E).

Circ_0007386 Promotes the Proliferation and Metastasis of HCC Cells in vivo

To assess the impact of circ_0007386 on the proliferation and metastasis of HCC in vivo, we designed a subcutaneous tumor model and a lung metastatic model. Tumor volume and weight in the subcutaneous tumor model were significantly reduced in the si-circ_0007386 group but increased in the overexpression group. (Figure 4A) The immunohistochemical staining results demonstrated decreased expression levels of Ki-67, N-cadherin, and vimentin in the circ_0007386 knockdown group. Conversely, elevated levels of E-cadherin were observed in this group. In contrast, the

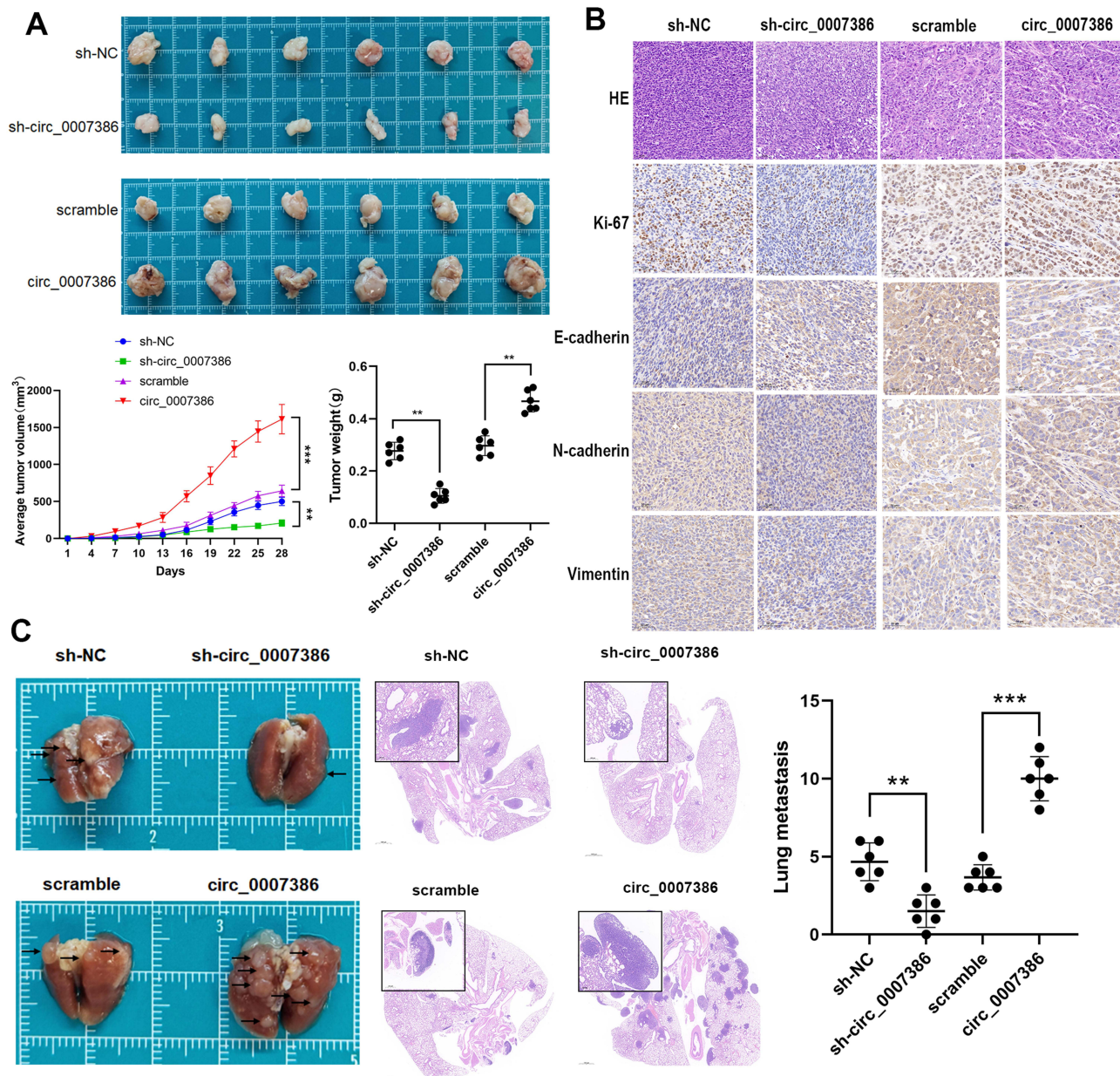


Figure 4 Circ_0007386 promotes the proliferation and metastasis of HCC cells in vivo. (A) Images of subcutaneous xenograft tumors (6 mice per group) in nude mice. The tumor volume and average weight were measured. (B) Immunohistochemical verification of the expression of HE, Ki67, E-cadherin, N-cadherin and Vimentin in tumors tissues. (C) Circ_0007386 stable knockdown or overexpression cells were used to generate lung metastasis. Lung metastatic nodules were stained with HE. The number of metastases was calculated. Data were all showed as mean \pm SD; ns indicated no significance, ** $p < 0.01$, *** $p < 0.001$.

circ_0007386 overexpression group exhibited the opposite result (Figure 4B). In the metastasis model, the down-regulation of circ_0007386 led to a reduction in the number and size of lung metastases, whereas the upregulation of circ_0007386 resulted in the opposite trend. (Figure 4C) This evidence indicates that circ_0007386 promoted HCC cell growth and metastasis in vivo.

Circ_0007386 Induces HCC Progression in a miR-507-Dependent Manner

Considering that circRNAs primarily act as sponges of miRNAs in the cytoplasm,^{13,14} we then predicted the possible circ_0007386-related miRNAs by two online databases (circBank and CircInteractome). As shown in Figure 5A, miR-507 and miR-567 were the potential targets of hsa-circ_0007386. Based on the PCR results, the expression of miR-507 in HCC tissues was lower than that in paracancerous tissues (Figure 5B) and was negatively correlated with circ_0007386 expression (Figure 5D). In a similar manner, the expression of miR-507 in HCC cells is lower than that in HHL-5 cells (Figure 5C). A higher level of circ_0007386 caused a lower level of miR-507 expression in Hep3B cells, while a lower level of circ_0007386 caused a higher level of miR-507 expression in MHCC97H cells (Figure 5E). A pull-down assay demonstrated that miR-507 could be pulled down by the circ0007386 probe (Figure 5F). The results from RNA immunoprecipitation (RIP) analysis using the AGO2 antibody showed that circ_0007386 and miR-507 were highly

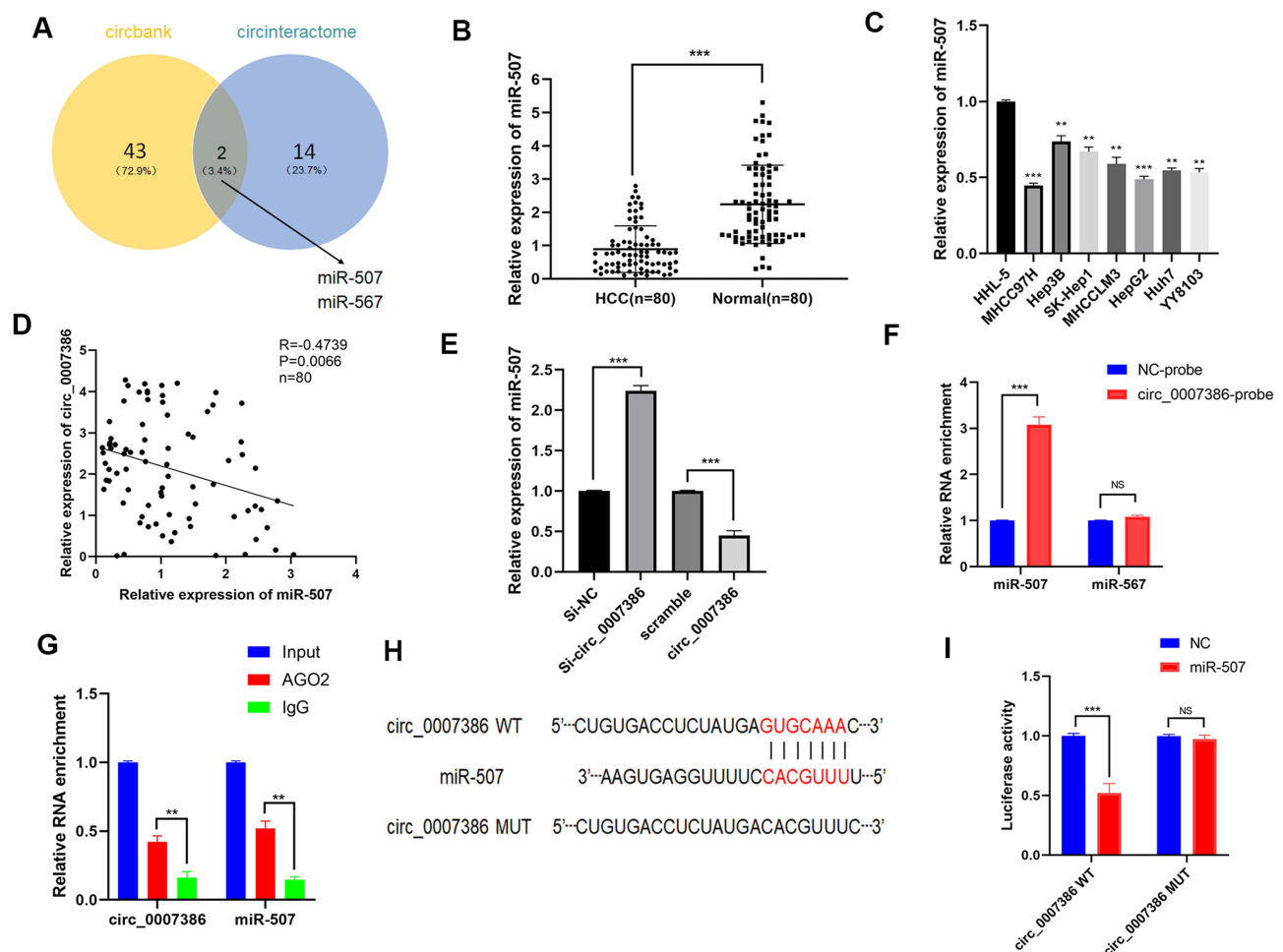


Figure 5 Circ_0007386 binds to miR-507 in HCC cells. (A) Venn diagram presented miRNAs of circ_0007386, based on circBank and CircInteractome. (B–C) The relative expression of miR-507 in HCC tissues and cells was determined using qRT-PCR. (D) Spearman correlation analysis of circ_0007386 expression versus miR-507 expression in HCC tissues. (E) The expression of miR-507 was upregulated upon circ_0007386 knockdown while being downregulated upon circ_0007386 overexpression. (F) Pull-down assay showed that miR-507 could be pulled down by the circ_0007386 probe. (G) RIP assay showed that circ_0007386 and miR-507 could be enriched by AGO2 antibody. (H) Wild-type (WT) and mutant plasmids (MUT) of circ_0007386 were designed according to the Starbase. (I) Luciferase activity in HCC cells confirmed the binding of circ_0007386 and miR-507. Data were all showed as mean \pm SD; ns indicated no significance, ** $p < 0.01$, *** $p < 0.001$.

enriched, indicating that circ_0007386 may have miRNA-related functions (Figure 5G). CircInteractome was employed to predict the binding sites between circ_0007386 and miR-507, and wild-type and mutant circ_0007386 vectors were constructed (Figure 5H). Subsequently, luciferase experiments were conducted to verify the binding affinity of the miRNA towards circ_0007386. HCC cells were transfected with a miR-507 mimic alongside wild-type and mutant circ_0007386 vectors with luciferase. After miR-507 overexpression, the luciferase activity of wild-type vectors was shown to be drastically decreased by approximately 50% (Figure 5I). MiR-567 does not exhibit any comparable impact (Figure S2A–C). Therefore, we conclude that miR-507 is a target miRNA of circ_0007386.

CCNT2 is a Direct Target of miR-507 and is Indirectly Regulated by Circ_0007386

In addition, we applied the miRDB, miRDIP, TargetScan, and miRTarBase databases to investigate the potential downstream targets of miR-507. The probable target gene of miR-507 was predicted to be Cyclin T2 (CCNT2) (Figures 6A and S3A–C). As circ_0007386 might stimulate tumor proliferation via CCNT2, we further analyzed CCNT2 expression in clinical samples.

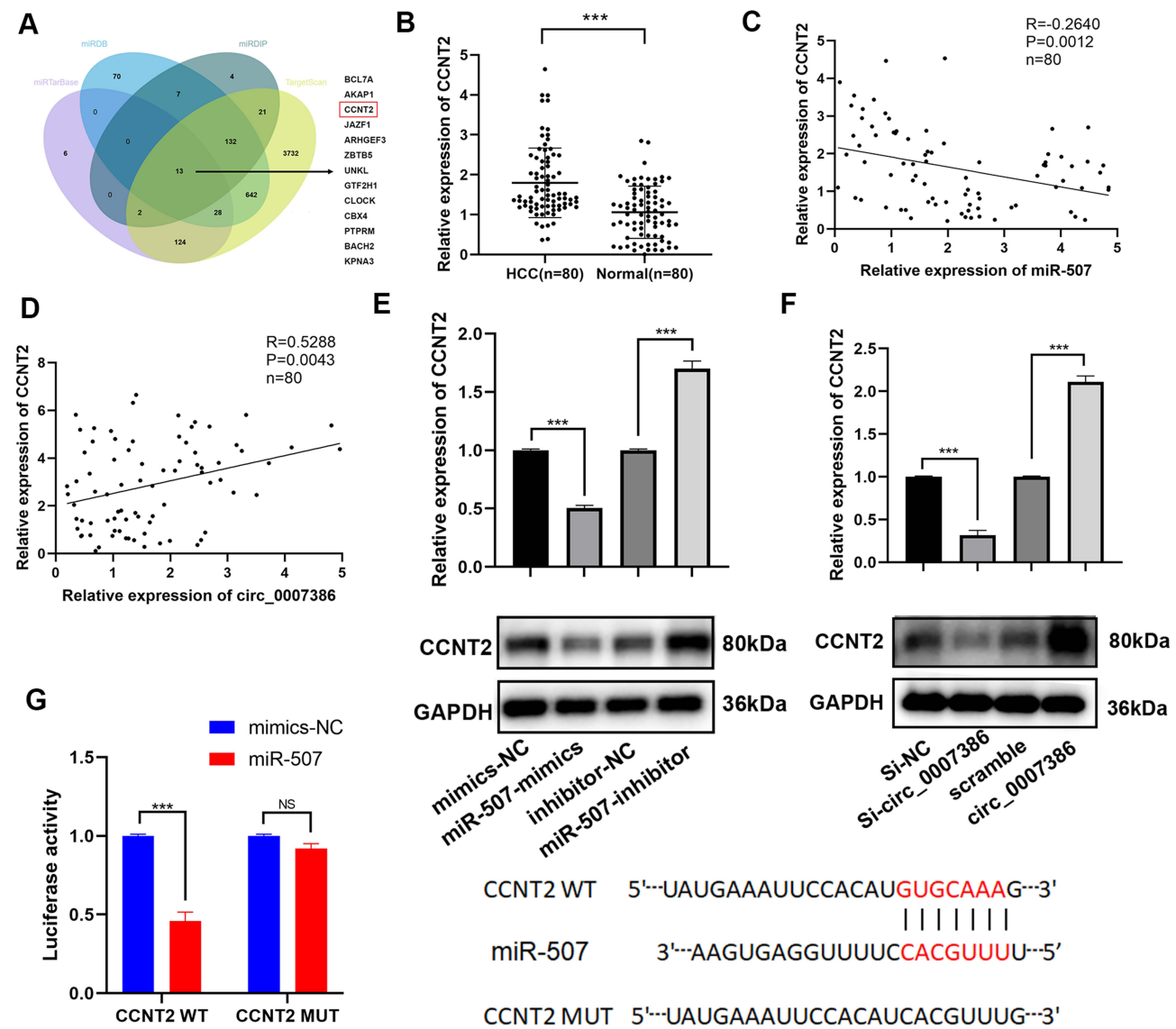


Figure 6 CCNT2 is a direct target of miR-507 in HCC. (A) Overlapped target genes of miR-507 predicted by miRDIP, TargetScan, miRDB and miRTarBase. (B) CCNT2 expression in HCC tissues compared to matched normal tissues (n = 80). (C–D) Spearman correlation analysis of miR-507 with CCNT2, and circ_0007386 with CCNT2 in HCC tissues. (E–F) CCNT2 were tested by Western blot in HCC cells after knockdown or overexpression of miR-507 and circ_0007386. (G) Relative luciferase activity were measured after co-transfection with CCNT2 3'UTR-WT or CCNT2 3'UTR-MUT and miR-507 mimics or mimics NC. Data were all showed as mean ± SD; ns indicated no significance, ***p < 0.001.

High expression of CCNT2 was observed in HCC tissues compared to paracancerous tissues, and was associated with elevated levels of circ_0007386 and reduced expression of miR-507 (Figure 6B–D). The results of Western blotting demonstrated that the overexpression of miR-507 led to a considerable decrease in the protein levels of CCNT2. In a similar manner, the depletion of circ_0007386 significantly repressed CCNT2 expression. On the other hand, the overexpression of circ_0007386 led to a substantial increase in the expression of CCNT2 (Figure 6E and F). To validate these results, we generated a luciferase reporter vector containing the wild type or mutant CCNT2 3' UTR binding site for miR-507. The luciferase activities of the wild-type CCNT2 3' UTR reporter were markedly diminished in hepatocellular carcinoma (HCC) cells that were transfected with the miR-507 mimic. Nonetheless, there was no substantial disparity observed in luciferase activity when the miR-507 mimic was cotransfected with the mutant CCNT2 3' UTR reporter (Figure 6G). These data indicate that CCNT2 can be regulated by miR-507 and circ_0007386.

Circ_0007386 Promoted HCC Progression Through the miR-507/CCNT2 Axis

To further explore the role of the circ_0007386/miR-507/CCNT2 axis in the development of HCC, we conducted a series of cellular functional experiments, such as the CCK-8 assay, colony formation and EdU assays, as well as Transwell and wound healing assays (Figures 7A–D and S4A). We observed that miR-507 knockdown could significantly restore the suppressive effects of circ_0007386 downregulation on HCC cell migratory and proliferation abilities, similar to CCNT2 overexpression. Furthermore, miR-507 suppression and CCNT2 overexpression significantly reversed the downregulation of CCNT2 expression and EMT induced by circ_0007386 downregulation (Figure S4B). These results indicate that circ_0007386 controls the expression of CCNT2 and promotes the migration and proliferation of HCC cells via miR-507.

Circ_0007386 Determines Lenvatinib Response in HCC

Two lenvatinib-resistant HCC cell lines, namely MHCC97H-LR and Hep-3B-LR, were generated to examine the potential role of circ_0007386 in the mediation of lenvatinib resistance in HCC. The IC₅₀ values of the two lenvatinib-resistant cell lines are notably larger compared to their respective parental cell lines. (Figure 8A). Following that, we used qRT-PCR to validate the constant upregulation of circ_0007386 in the two lenvatinib-resistant cell lines compared to their respective parental cell lines (Figure 8B). To examine the associations between circ_0007386 and the development of lenvatinib resistance in HCC, we proceeded to suppress the expression of circ_0007386 in MHCC97H-LR and Hep-3B-LR cells. Subsequently, we confirmed the effectiveness of the knockdown procedure (Figure 8C). CCK-8 and colony formation assay revealed that circ_0007386 knockdown significantly enhanced the lenvatinib sensitivity of the two lenvatinib-resistant HCC cell lines (Figure 8D and E). Collectively, these data suggested a potential mechanistic correlation between circ_0007386 and resistance to lenvatinib in HCC.

Discussion

According to previous reports, circRNAs /miRNAs axis have received much attention for their role in the diagnosis, tumor microenvironment, treatment and drug resistance of HCC.^{15,16} Huang et al¹⁷ showed that circMET is an onco-circRNA that induces HCC development and immune tolerance via the Snail/DPP4/CXCL10 axis. Fu et al¹⁸ reported that microRNA-223 attenuates hepatocarcinogenesis by blocking hypoxia-driven angiogenesis and immunosuppression. CircRNAs derived from CRIM1 have different roles in multiple tumors; for instance, one of them functions as a ceRNA to promote nasopharyngeal carcinoma metastasis and docetaxel chemoresistance.⁹ In another report, circ_0002346 inhibited tumor immune evasion through a competitive combination with IGF2BP1 to mediate non-small cell lung cancer immune evasion.¹⁹ Even in HCC, circCRIM1 (hsa_circ_0002346) has been reported to be a ceRNA that promotes HCC proliferation and angiogenesis.¹² In general, CRIM1-derived circRNAs play an important role in cancers, and some have even become therapeutic targets or prognostic factors; however, their roles in HCC have not been fully elucidated. In this investigation, we showed the important roles and mechanisms of circ_0007386 in the development of HCC and stress its prognostic and therapeutic value in the metastasis and progression of HCC.

CircRNAs are an abundant family of mainly noncoding RNA molecules that have evolved over the past decade. Numerous circRNAs play critical roles in cancer formation and progression via a wide variety of methods. Initially, it was discovered that circRNA can regulate the production of its linear RNA counterpart competitively. Recent studies have also revealed other

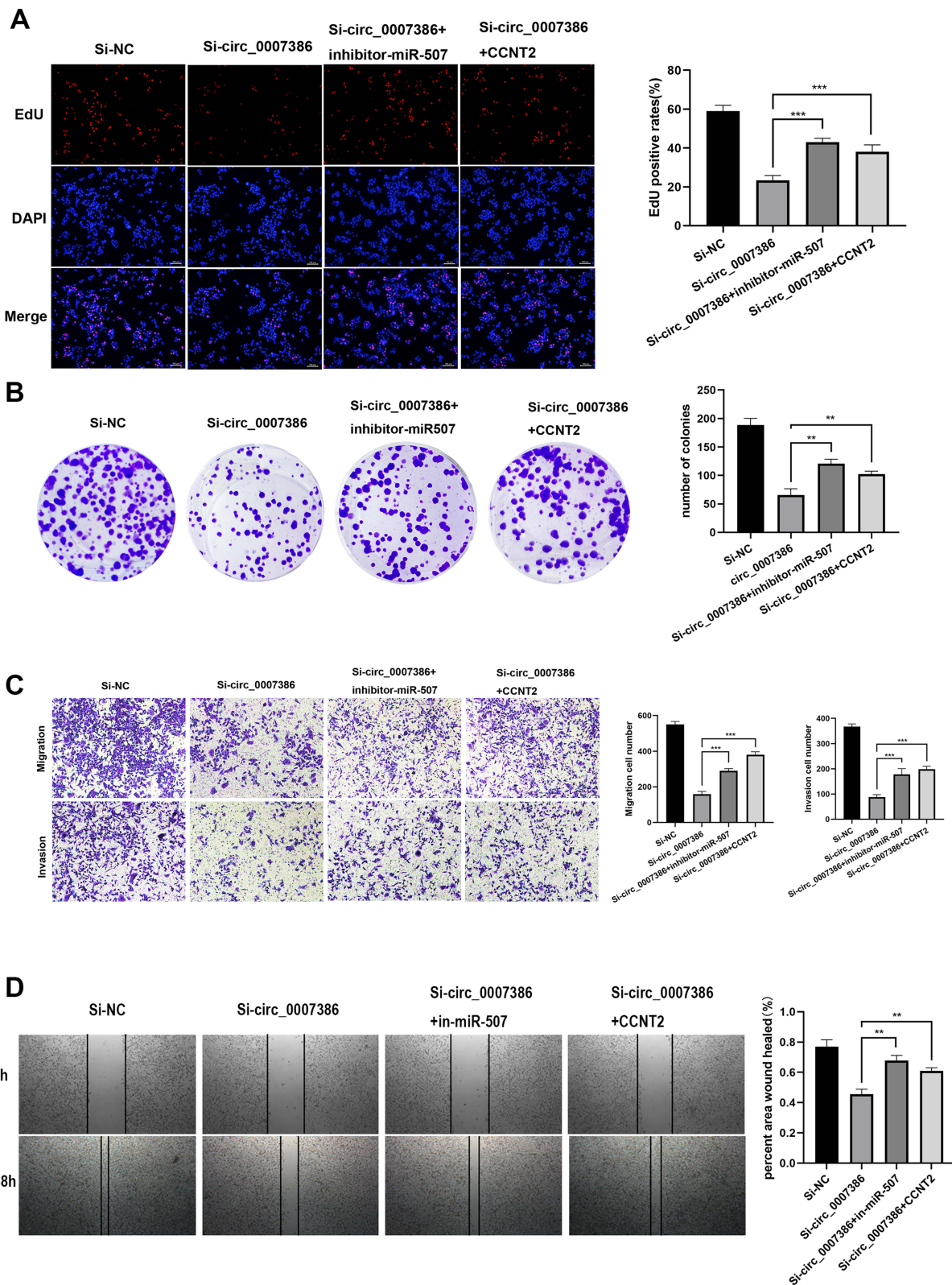


Figure 7 The function of the circ_0007386/miR-507/CCNT2 axis in HCC was verified by rescue experiments. **(A and B)** The EdU assay and colony formation assays were used to assess the proliferative potential of various groups. **(C and D)** The Transwell assay and wound healing assays was used to test the capacity of HCC cells to migrate and invade in different groups. Data were all showed as mean ± SD; ns indicated no significance, **p < 0.01, ***p < 0.001.

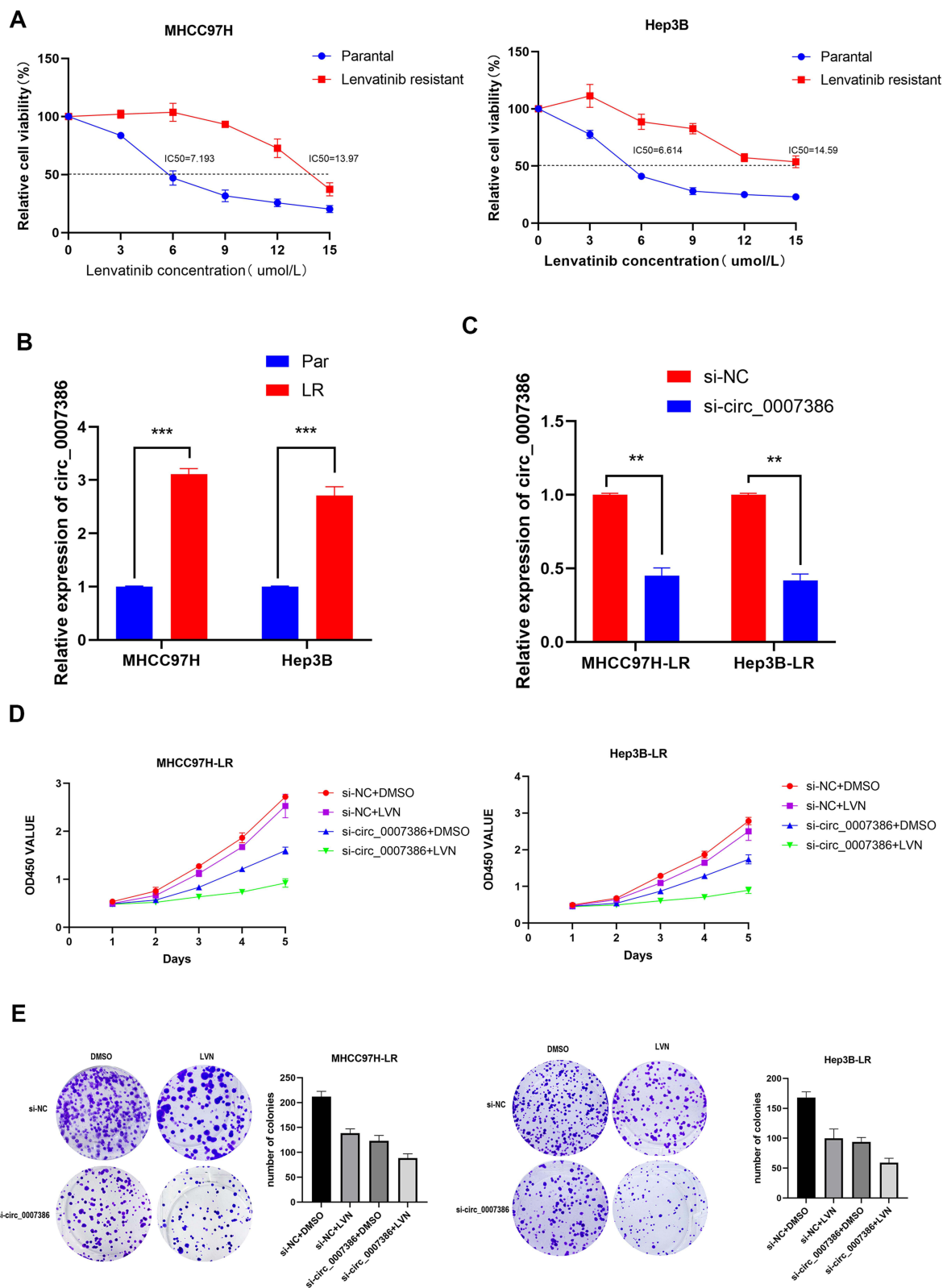


Figure 8 Knockdown of circ_0007386 inhibited lenvatinib resistance of HCC cells. **(A)** Cells were treated with lenvatinib for 48 hours, and their cell survival curves and IC50 were calculated by CCK-8 assay. **(B)** The level of circ_0007386 in the two lenvatinib-resistant HCC cell lines was measured by qRT-PCR. **(C)** The knockdown efficiency of circ_0007386 in the two lenvatinib-resistant HCC cell lines was measured by qRT-PCR. **(D–E)** The CCK-8 and colony formation assays were used to assess the effect of circ_0007386 knockdown on lenvatinib resistance. Data were all showed as mean ± SD; ns indicated no significance, **p < 0.01, ***p < 0.001.

capabilities of circRNAs: some circRNAs bind to microRNAs, others are translated, and it has been demonstrated that circRNAs regulate the immune system. Furthermore, circular RNAs (circRNAs) have significant promise as biomarkers for prognosis, diagnosis, and recurrence, as evidenced by their detectability in liquid biopsy specimens, including plasma and saliva. However, only a few circRNAs have been identified, and their involvement in HCC is mainly unclear.^{20–22}

In this study, we revealed that circ_0007386 is upregulated in HCC tissues and cell lines. The findings from functional assays provided evidence supporting the notion that increased expression of circ_0007386 facilitated the metastasis of HCC cells and promoted their proliferation. Subsequently, we investigated the fundamental mechanism and clinical significance of circ_0007386 in HCC.

CircRNAs have been demonstrated to act as ceRNAs for miRNAs and then regulate downstream target genes competitively. Recent studies have indicated that some circRNAs can modulate carcinogenesis and cancer development in a ceRNA manner.^{23–25} In our research, circ_0007386, with stable and high cytoplasmic expression is the promising ceRNA in HCC cells. Additional experiments demonstrated that circ_0007386 can directly bind to and inhibit the activity of miR-507. According to previous research, miR-507 may serve as a tumor inhibitor in various cancers, including non-small cell lung cancer, breast cancer and gastric carcinoma,^{26–28} nonetheless, its role in HCC must be clarified.

Cyclin T2 (CCNT2) is a conserved cyclin family member with a notable periodicity in protein abundance across the cell cycle. In a previous study, CCNT2 was linked to cell proliferation and the advancement of various carcinomas, including HCC and laryngeal papilloma.^{29,30} It is known that some miRNAs regulate gene expression by binding directly to the 3' UTR of target mRNAs, resulting in mRNA degradation or translation inhibition. In the current research, circ_0007386 prevented miR-507 from inhibiting CCNT2 expression. In practice, CCNT2 overexpression reversed the si-circ_0007386-mediated inhibition of HCC cell migration and EMT. Consequently, the circ_0007386/miR-507/CCNT2 axis may be a key regulator in the development of HCC.

Since its approval in 2018, lenvatinib has been used for the treatment of HCC. Nevertheless, the effectiveness of lenvatinib is impeded by the emergence of drug resistance, which poses a substantial obstacle. Consequently, it is essential to comprehend the precise mechanisms underlying chemoresistance. Available research suggests that circRNAs are crucial in resistance to lenvatinib.^{31–33} Since Hong et al demonstrate that circCRIM1 functions as a ceRNA to promote nasopharyngeal docetaxel chemoresistance;⁹ Shinsuke Yamamoto et al³⁴ showed that their in vitro analysis revealed that the transfection of miR-507 led to an increase in the sensitivity of cell-growth suppression with cisplatin (CDDP) in A549 cells; Xu et al³⁵ demonstrated that CCNT2-AS1 and SNHG1/ has-miR-204-5p/STIL axis were more sensitive to the gemcitabine, doxorubicin, while more resistant to the sorafenib and sunitinib. We consider that the circ_0007386/miR-507/CCNT2 axis is related to HCC chemosensitivity. As speculated, the expression of circ_0007386 is higher in lenvatinib-resistant cell lines compared to their parental cells. Furthermore, the knockdown of circ_0007386 enhanced the sensitivity to lenvatinib, suggesting that circ_0007386 plays a crucial role in the development of lenvatinib resistance.

Conclusions

In conclusion, our research shows that circ_0007386 competitively sponges miR-507 to inhibit the suppression effect of miR-507 on CCNT2 and then contributes to HCC cell proliferation, metastasis, EMT and lenvatinib resistance. These results offer new perspectives on comprehending the advancement and treatment of HCC, as well as viable prognostic and therapeutic approaches for individuals diagnosed with HCC.

Funding

This work was supported by grants from the National Natural Science Foundation of China (81871260); Health Research Projects of Jiangsu Provincial Health Committee (H2019045); The training program of “Double hundred” young and middle-aged medical and health talents in Wuxi (BJ020034); Key research and development Projects of Anhui Province (2022e07020048); Young Scholars Fostering Fund of the First Affiliated Hospital of Nanjing Medical University (PY2022007).

Disclosure

The authors report no conflicts of interest in this work.

References

1. Huang DQ, El-Serag HB, Loomba R. Global epidemiology of NAFLD-related HCC: trends, predictions, risk factors and prevention. *Nat Rev Gastroenterol Hepatol*. 2021;18(4):223–238. doi:10.1038/s41575-020-00381-6
2. Sung H, Ferlay J, Siegel RL, et al. Global cancer statistics 2020: globocan estimates of incidence and mortality worldwide for 36 cancers in 185 countries. *CA Cancer J Clin*. 2021;71(3):209–249. doi:10.3322/caac.21660
3. Armakola M, Higgins MJ, Figley MD, et al. Inhibition of RNA lariat debranching enzyme suppresses TDP-43 toxicity in ALS disease models. *Nat Genet*. 2012;44(12):1302–1309. doi:10.1038/ng.2434
4. Zheng Q, Bao C, Guo W, et al. Circular RNA profiling reveals an abundant circHIPK3 that regulates cell growth by sponging multiple miRNAs. *Nat Commun*. 2016;7(1):11215. doi:10.1038/ncomms11215
5. Chen R, Wang SK, Belk JA, et al. Engineering circular RNA for enhanced protein production. *Nat Biotechnol*. 2023;41(2):262–272. doi:10.1038/s41587-022-01393-0
6. Xue C, Li G, Zheng Q, et al. The functional roles of the circRNA/Wnt axis in cancer. *Mol Cancer*. 2022;21(1):108. doi:10.1186/s12943-022-01582-0
7. Lei M, Zheng G, Ning Q, Zheng J, Dong D. Translation and functional roles of circular RNAs in human cancer. *Mol Cancer*. 2020;19(1):30. doi:10.1186/s12943-020-1135-7
8. Wang J, Zhao X, Wang Y, et al. circRNA-002178 act as a ceRNA to promote PDL1/PD1 expression in lung adenocarcinoma. *Cell Death Dis*. 2020;11(1):32. doi:10.1038/s41419-020-2230-9
9. Hong X, Liu N, Liang Y, et al. Circular RNA CRIM1 functions as a ceRNA to promote nasopharyngeal carcinoma metastasis and docetaxel chemoresistance through upregulating FOXQ1. *Mol Cancer*. 2020;19(1):33. doi:10.1186/s12943-020-01149-x
10. Du Y, Liu X, Zhang S, et al. CircCRIM1 promotes ovarian cancer progression by working as ceRNAs of CRIM1 and targeting miR-383-5p/ZEB2 axis. *Reprod Biol Endocrinol*. 2021;19(1):176. doi:10.1186/s12958-021-00857-3
11. Yu XY, Ma CQ, Sheng YH. circRNA CRIM1 regulates the migration and invasion of bladder cancer by targeting miR182/Foxo3a axis. *Clin Transl Oncol*. 2022;24(6):1195–1203. doi:10.1007/s12094-021-02768-6
12. Ji Y, Yang S, Yan X, et al. CircCRIM1 promotes hepatocellular carcinoma proliferation and angiogenesis by sponging miR-378a-3p and regulating SKP2 expression. *Front Cell Dev Biol*. 2021;9:796686. doi:10.3389/fcell.2021.796686
13. Shang A, Gu C, Wang W, et al. Exosomal circPACRGL promotes progression of colorectal cancer via the miR-142-3p/miR-506-3p- TGF- β 1 axis. *Mol Cancer*. 2020;19(1):117. doi:10.1186/s12943-020-01235-0
14. Cen J, Liang Y, Huang Y, et al. Circular RNA circSDHC serves as a sponge for miR-127-3p to promote the proliferation and metastasis of renal cell carcinoma via the CDKN3/E2F1 axis. *Mol Cancer*. 2021;20(1):19. doi:10.1186/s12943-021-01314-w
15. Zhou Y, Mao X, Peng R, Bai D. CircRNAs in hepatocellular carcinoma: characteristic, functions and clinical significance. *Int J Med Sci*. 2022;19(14):2033–2043. doi:10.7150/ijms.74713
16. Xiong D, He R, Dang Y, et al. The latest overview of circRNA in the progression, diagnosis, prognosis, treatment, and drug resistance of hepatocellular carcinoma. *Front Oncol*. 2020;10:608257. doi:10.3389/fonc.2020.608257
17. Huang XY, Zhang P-F, Wei C-Y, et al. Circular RNA circMET drives immunosuppression and anti-PD1 therapy resistance in hepatocellular carcinoma via the miR-30-5p/snail/DPP4 axis. *Mol Cancer*. 2020;19(1):92. doi:10.1186/s12943-020-01213-6
18. Fu Y, Mackowiak B, Feng D, et al. MicroRNA-223 attenuates hepatocarcinogenesis by blocking hypoxia-driven angiogenesis and immunosuppression. *Gut*. 2023;72(10):1942–1958. doi:10.1136/gutjnl-2022-327924
19. Peng W, Ye L, Xue Q, et al. Silencing of circCRIM1 Drives IGF2BP1-Mediated NSCLC Immune Evasion. *Cells*. 2023;12(2):273. doi:10.3390/cells12020273
20. Patop IL, Wüst S, Kadener S. Past, present, and future of circRNAs. *EMBO j*. 2019;38(16):e100836. doi:10.15252/embj.2018100836
21. Kristensen LS, Jakobsen T, Hager H, Kjems J. The emerging roles of circRNAs in cancer and oncology. *Nat Rev Clin Oncol*. 2022;19(3):188–206. doi:10.1038/s41571-021-00585-y
22. Zhou WY, Cai Z-R, Liu J, et al. Circular RNA: metabolism, functions and interactions with proteins. *Mol Cancer*. 2020;19(1):172. doi:10.1186/s12943-020-01286-3
23. Xue Q, Huang Y, Chang J, et al. CircRNA-mediated ceRNA mechanism in Osteoarthritis: special emphasis on circRNAs in exosomes and the crosstalk of circRNAs and RNA methylation. *Biochem Pharmacol*. 2023;212:115580. doi:10.1016/j.bcp.2023.115580
24. Cheng Z, Yu C, Cui S, et al. circTP63 functions as a ceRNA to promote lung squamous cell carcinoma progression by upregulating FOXM1. *Nat Commun*. 2019;10(1):3200. doi:10.1038/s41467-019-11162-4
25. Zhou J, Wang L, Sun Q, et al. Hsa_circ_0001666 suppresses the progression of colorectal cancer through the miR-576-5p/PCDH10 axis. *Clin Transl Med*. 2021;11(11):e565. doi:10.1002/ctm2.565
26. Li J, Zhu Z, Li S, et al. Circ_0089823 reinforces malignant behaviors of non-small cell lung cancer by acting as a sponge for microRNAs targeting SOX4. *Neoplasia*. 2021;23(9):887–897. doi:10.1016/j.neo.2021.06.011
27. Fang X, Pan A. MiR-507 inhibits the progression of gastric carcinoma via targeting CBX4-mediated activation of Wnt/ β -catenin and HIF-1 α pathways. *Clin Transl Oncol*. 2022;24(10):2021–2028. doi:10.1007/s12094-022-02862-3
28. Jia L, Liu W, Cao B, Li H, Yin C. MiR-507 inhibits the migration and invasion of human breast cancer cells through Flt-1 suppression. *Oncotarget*. 2016;7(24):36743–36754. doi:10.18632/oncotarget.9163
29. Zhao D, Hou Y. Long non-coding RNA nuclear-enriched abundant transcript 1 (LncRNA NEAT1) upregulates Cyclin T2 (CCNT2) in laryngeal papilloma through sponging miR-577/miR-1224-5p and blocking cell apoptosis. *Bioengineered*. 2022;13(1):1828–1837. doi:10.1080/21655979.2021.2017653
30. Meng H, Li R, Xie Y, et al. Nanoparticles Mediated circROBO1 Silencing to Inhibit Hepatocellular Carcinoma Progression by Modulating miR-130a-5p/CCNT2 Axis. *Int J Nanomed*. 2023;18:1677–1693. doi:10.2147/ijn.S399318
31. Hao X, Zhang Y, Shi X, et al. CircPAK1 promotes the progression of hepatocellular carcinoma via modulation of YAP nucleus localization by interacting with 14-3-3 ζ . *J Exp Clin Cancer Res*. 2022;41(1):281. doi:10.1186/s13046-022-02494-z
32. Liu D, Liu W, Chen X, et al. circKCNN2 suppresses the recurrence of hepatocellular carcinoma at least partially via regulating miR-520c-3p/methyl-DNA-binding domain protein 2 axis. *Clin Transl Med*. 2022;12(1):e662. doi:10.1002/ctm2.662

33. Zhang P, Sun H, Wen P, et al. circRNA circMED27 acts as a prognostic factor and mediator to promote lenvatinib resistance of hepatocellular carcinoma. *Mol Ther Nucleic Acids*. 2022;27:293–303. doi:10.1016/j.omtn.2021.12.001
34. Yamamoto S, Inoue J, Kawano T, et al. The impact of miRNA-based molecular diagnostics and treatment of NRF2-stabilized tumors. *Mol Cancer Res*. 2014;12(1):58–68. doi:10.1158/1541-7786.Mcr-13-0246-t
35. Xu L, Zhang S, Feng J, et al. ncRNAs-mediated overexpression of STIL predict unfavorable prognosis and correlated with the efficacy of immunotherapy of hepatocellular carcinoma. *Cancer Cell Int*. 2023;23(1):44. doi:10.1186/s12935-023-02869-y

Journal of Hepatocellular Carcinoma

Dovepress

Publish your work in this journal

The Journal of Hepatocellular Carcinoma is an international, peer-reviewed, open access journal that offers a platform for the dissemination and study of clinical, translational and basic research findings in this rapidly developing field. Development in areas including, but not limited to, epidemiology, vaccination, hepatitis therapy, pathology and molecular tumor classification and prognostication are all considered for publication. The manuscript management system is completely online and includes a very quick and fair peer-review system, which is all easy to use. Visit <http://www.dovepress.com/testimonials.php> to read real quotes from published authors.

Submit your manuscript here: <https://www.dovepress.com/journal-of-hepatocellular-carcinoma-journal>